

**Electronic Supplementary Information (ESI)**

**Coordination Polymer Derived  $\text{Co}_3\text{O}_4/\text{Co-N@NMC}$  Composite Material as Zn-air  
Battery Cathode Electrocatalyst and Microwave Absorber**

Yaqin Wang,<sup>a</sup> Xinxin Xu,<sup>\*a</sup> Luyao Liu,<sup>a</sup> Jin Chen<sup>\*b</sup> and Guimei Shi<sup>\*c</sup>

<sup>a</sup> Department of Chemistry, College of Science, Northeastern University, Shenyang  
110819, China

<sup>b</sup> Key Laboratory of Electromagnetic Processing of Materials (Ministry of Education),  
Northeastern University, Shenyang, Liaoning 110819, People's Republic of China

<sup>c</sup> College of Science, Shenyang University of Technology, No. 111, Shenliao West  
Road, Economic & Technological Development Zone, Shenyang, 110870, P. R. China

## Materials and characterization

All chemicals were of analytical grade, commercially available from Sinopharm Chemical Reagent Co. Ltd (Shanghai, China) and used as received without further purification. Suitable single crystal of **CoCP** was carefully selected under an optical microscope and glued on a glass fiber. Structural measurement was performed on a Bruker AXS SMART APEX II CCD diffractometer at 293 K (1864421). The morphology was observed on an ultra plus field emission scanning electron microscope (SEM, ultra plus, ZEISS) and a transmission electron microscopy (TEM, JEOL, JEM-2100F). PXRD patterns were recorded on X-ray diffractometer with Cu KR ( $\lambda=1.5418 \text{ \AA}$ ) radiation (Philips X'Pert Pro Super, Philips). Raman spectroscopy was conducted with an excitation wavelength of 633 nm (LabRAMHR-800, HORIBA). N<sub>2</sub> sorption analysis was conducted using an ASAP 2020 accelerated surface area and a porosimetry instrument (Micromeritics, Norcross, GA), equipped with an automated surface area, at 77 K using Barrett-Emmett-Teller (BET) calculations for the surface area. The pore size distribution plot was based on the original density functional theory model. XPS was performed with Mg K $\alpha$  radiation (1253.6 eV) as an excitation source (ESCALab MKII, Thermo Scientific, Waltham, MA). Electrochemical experiments were conducted on CHI-660E electrochemical workstation. The LAND-CT2001A testing devices were used to analyze the battery discharge/charge performance.

### Synthesis of [Co<sub>1.5</sub>(tmc)(bipy)(H<sub>2</sub>O)<sub>3</sub>] $\cdot$ 2H<sub>2</sub>O (CoCP)

At first, H<sub>3</sub>tmc (0.021 g, 0.1 mmol) and bipy (0.018 g, 0.1 mmol) ligands were dispersed in 10 mL water. Then, Co(OAc)<sub>2</sub> $\cdot$ 4H<sub>2</sub>O (0.049 g, 0.2 mmol) was added in this solution slowly. Finally the pH value of this solution was adjusted to 4.5 with 1.0 M KOH. After stirred for 30 min, the solution was poured into a Teflonlined reactor

(20 mL). The reactor was heated at 150 °C for 72 h and cooled to room temperature with the rate 15 °C·h<sup>-1</sup>. A lot of red crystals were synthesized, with the yield 80 % (based on Co).

### **Synthesis of Co<sub>3</sub>O<sub>4</sub>/Co-N@NMC composite material**

With an agate mortar and pestle, the crystals of **CoCP** (0.8 g) were ground for 30 min. The resulted powder was transferred into a tube furnace and heated with the rate 3 °C·min<sup>-1</sup> to 400°C. The calcination of **CoCP** was protected with N<sub>2</sub> gas flow for 3 h. The products were gathered and washed with water, ethanol for three times. Then transferred in the oven and dried for 10 h at 70 °C.

### **Electrochemical measurements**

ORR was performed in O<sub>2</sub> saturated 0.1 M KOH, while OER measurements were conducted in an N<sub>2</sub> saturated 1.0 M KOH solution. In ORR, linear sweep voltammetry (LSV) curves were recorded at 5 mV·s<sup>-1</sup>. Different rotating speeds of the RDE, including 800, 1000, 1200, 1400, 1600, 1800 and 2000 rpm revolutions per minute (rpm), were employed for the ORR measurements. Cyclic voltammetry (CV) cycling was carried out from 0 to 1.2 V versus RHE a scanning rate of 10 mV·s<sup>-1</sup>. In OER, LSV curves were also measured at 5 mV·s<sup>-1</sup>. The potential vs. RHE was calibrated using the following equation:  $E(\text{vs. RHE}) = E(\text{vs. SCE}) + 0.059 \times \text{pH} + 0.241 \text{ V}$ . In ORR, the electron transfer number was determined by using the Koutechy-Levich (K-L) equation (Eq. 1). In this equation  $j$  is the measured current density,  $j_k$  is the kinetic current density, and  $\omega$  is the electrode rotating rate. The parameter  $B$  could be calculated from the slope of the K-L plots based on the following Levich equation (Eq. 2), in which  $n$  is the electron transfer number per oxygen molecule,  $F$  is the Faraday constant ( $F = 96485 \text{ C}\cdot\text{mol}^{-1}$ ),  $D_0$  is the diffusion coefficient of O<sub>2</sub> in 0.1 M KOH ( $D_0 =$

$1.9 \times 10^{-5} \text{ cm}^2\cdot\text{s}^{-1}$ ),  $\nu$  is the kinetic viscosity ( $\nu = 0.01 \text{ cm}^2\cdot\text{s}^{-1}$ ), and  $C_0$  is the bulk concentration of  $\text{O}_2$  ( $C_0 = 1.2 \times 10^{-6} \text{ mol}\cdot\text{cm}^{-3}$ ). The value 0.2 is applied when the rotation speed is expressed in rpm. Electrochemical impedance spectroscopy (EIS) measurements were carried out from 100 kHz to 100 mHz.

$$1/j = 1/j_k + 1/B\omega^{1/2} \quad (1)$$

$$B = 0.62nF(D_0)^{2/3}(V)^{-1/6}C_0 \quad (2)$$

### **Zn-air battery assembly**

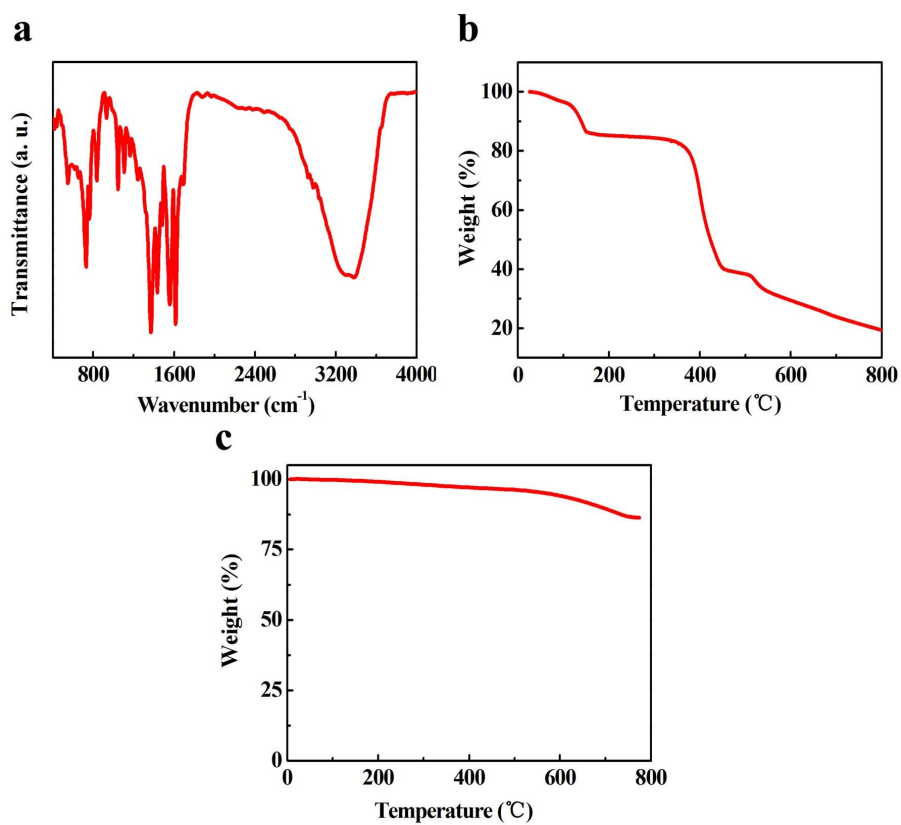
At first, the powder of **Co<sub>3</sub>O<sub>4</sub>/Co-N@NMC** (10 mg) was dispersed in the solution of ethanol (960  $\mu\text{L}$ ) and Nafion (40  $\mu\text{L}$ ). The resulted ink was cast on carbon fiber paper. The average catalyst loading mass is about  $1.8 \text{ mg}\cdot\text{cm}^{-2}$ . With this electrode as air cathode and zinc plate as anode, the Zn-air battery was assembled. In this battery, the mixed solution of KOH (6.0 M) and  $\text{ZnCl}_2$  (0.2 M) was employed as electrolyte.

Table S1. Bond lengths [Å] and angles [°] for **CoCP**

Co(1)-O(5)	2.0662(17)	Co(1)-O(5)#1	2.0662(17)
Co(1)-O(8)	2.144(2)	Co(1)-O(8)#1	2.144(2)
Co(1)-O(9)	2.092(2)	Co(1)-O(9)#1	2.092(2)
Co(2)-O(1)#2	2.0852(19)	Co(2)-O(3)	2.0668(17)
Co(2)-O(7)	2.0776(19)	Co(2)-N(1)	2.148(2)
Co(2)-N(2)	2.098(2)		
O(5)#1-Co(1)-O(5)	180.00(12)	O(5)#1-Co(1)-O(9)#1	91.76(8)
O(5)-Co(1)-O(9)#1	88.24(8)	O(5)#1-Co(1)-O(9)	88.24(8)
O(5)-Co(1)-O(9)	91.76(8)	O(9)#1-Co(1)-O(9)	180.000(1)
O(5)#1-Co(1)-O(8)#1	89.10(8)	O(5)-Co(1)-O(8)#1	90.90(8)
O(9)#1-Co(1)-O(8)#1	93.45(9)	O(9)-Co(1)-O(8)#1	86.55(9)
O(5)#1-Co(1)-O(8)	90.90(8)	O(5)-Co(1)-O(8)	89.10(8)
O(9)#1-Co(1)-O(8)	86.55(9)	O(9)-Co(1)-O(8)	93.45(9)
O(8)#1-Co(1)-O(8)	180.0	O(3)-Co(2)-O(7)	95.85(8)
O(3)-Co(2)-O(1)#2	91.99(7)	O(1)#2-Co(2)-N(2)	140.43(8)
O(7)-Co(2)-O(1)#2	96.35(8)	O(3)-Co(2)-N(1)	88.70(8)
O(3)-Co(2)-N(2)	122.74(8)	O(7)-Co(2)-N(1)	174.38(8)
O(7)-Co(2)-N(2)	98.04(8)	O(1)#2-Co(2)-N(1)	86.75(8)
N(2)-Co(2)-N(1)	76.68(9)		

Symmetry transformations used to generate equivalent atoms: #1: -x+2, -y+1, -z+1;

#2: x+1, y, z



**Fig. S1** (a) FTIR of **CoCP**; (b) TGA of **CoCP**; (c) TGA of **Co<sub>3</sub>O<sub>4</sub>/Co-N@NMC**

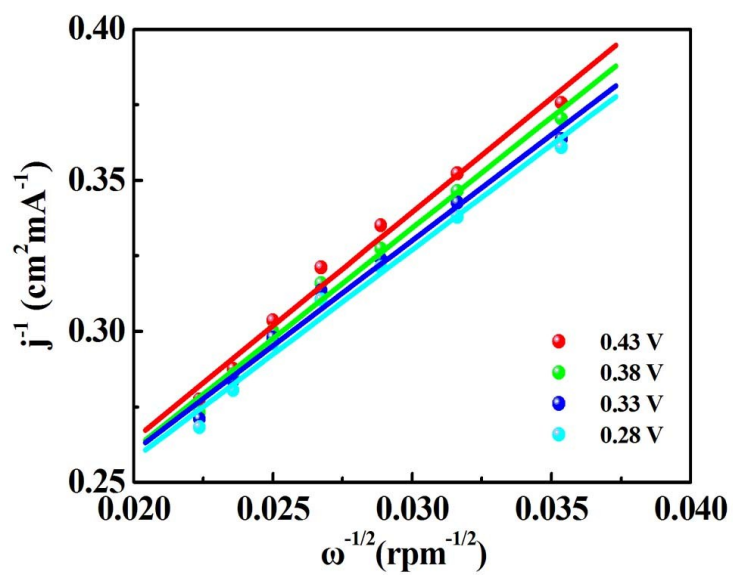


**Fig. S2** Koutecky-Levich plots of oxygen reduction at different potentials for  $\text{Co}_3\text{O}_4/\text{Co-N@NMC}$

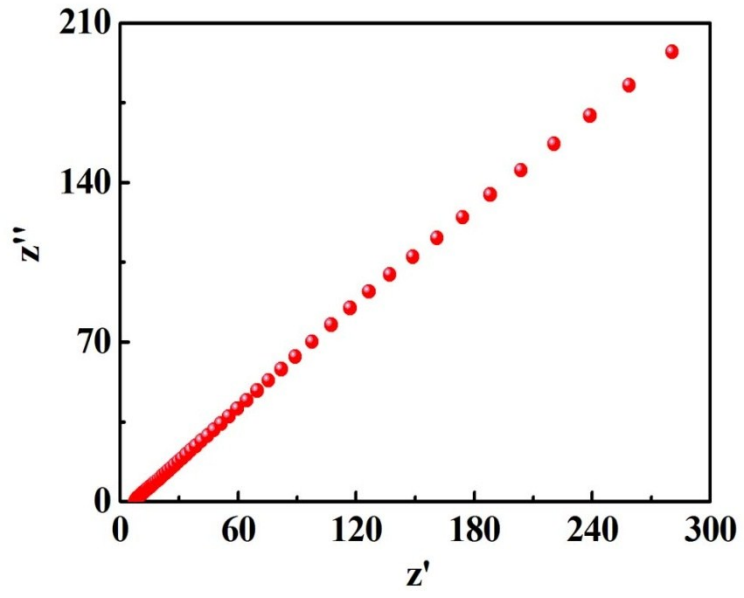


Fig. S3 the EIS of  $\text{Co}_3\text{O}_4/\text{Co-N@NMC}$